



# Effect of soldering condition on formation of intermetallic phases developed between Sn–0.3Ag–0.7Cu low-silver lead-free solder and Cu substrate

Niwat Mookam<sup>a</sup>, Kannachai Kanlayasiri<sup>b,\*</sup>

<sup>a</sup> Department of Industrial Engineering Technology, Rajamangala University of Technology Rattanakosin, Wang Klai Kangwon Campus, Prachuapkhirikhan 77110, Thailand

<sup>b</sup> Department of Industrial Engineering, King Mongkut's Institute of Technology Ladkrabang, Bangkok 10520, Thailand

## ARTICLE INFO

### Article history:

Received 5 January 2011

Received in revised form 1 March 2011

Accepted 6 March 2011

Available online 12 March 2011

### Keywords:

Metals and alloys

Intermetallics

Mechanical properties

Microstructure

## ABSTRACT

In this paper, effect of soldering time and temperature on formation of intermetallic compounds developed between Sn–0.3Ag–0.7Cu lead-free solder and copper substrate was investigated. Dip soldering was performed at 250, 270, and 290 °C with soldering time of 5, 10, 15, and 20 s. Either  $\epsilon$ -Cu<sub>3</sub>Sn or  $\eta$ -Cu<sub>6</sub>Sn<sub>5</sub> intermetallic phase was found at the interface between the solder and the substrate depending on the soldering condition, i.e., soldering time and soldering temperature.  $\epsilon$ -Cu<sub>3</sub>Sn was found only when the substrate was soldered at 250 °C for 5 and 10 s. At other soldering conditions, only  $\eta$ -Cu<sub>6</sub>Sn<sub>5</sub> was found at the interfacial zone. Crystal structure of  $\epsilon$ -Cu<sub>3</sub>Sn intermetallic phase was orthorhombic, and it was hexagonal structure for  $\eta$ -Cu<sub>6</sub>Sn<sub>5</sub>. Transformation of the intermetallic phases was also discussed.

© 2011 Elsevier B.V. All rights reserved.

## 1. Introduction

The RoHS directive legislated by the European Union forces electronics industry to use Pb-free solders in an effort to reduce the toxic substance. There are many Pb-free solders that are of interest such as, Sn–Ag, Sn–Cu, Sn–Zn, and Sn–Ag–Cu alloys. The Sn–Ag–Cu family of alloys is a very attractive candidate because of its advantages in mechanical properties and its good soldering ability [1–4]. Sn–0.3Ag–0.7Cu solder is a low-Ag lead-free solder alloy in the SAC family. This solder possesses a major advantage in that it provides a thinner brittle Ag<sub>3</sub>Sn intermetallic layer during soldering process due to its low-Ag content [5,6]. Moreover, cost of Sn–0.3Ag–0.7Cu solder is relatively low in the SAC family as a result of its low-Ag content.

There are many soldering processes have been used to make soldered joints such as hand soldering, dip soldering, and wave soldering [7]. During a soldering process, molten solder reacts with the substrate, and intermetallic compounds are formed at the interfacial zone between the solder and the substrate. Understanding of formation of the intermetallic phases during the soldering process is very important because the intermetallic compounds formed at the interface play an important role to reliability of the soldered joint during its service period [8]. Mechanical properties of the

intermetallic phases directly affect fatigue life, shear strength, and tensile strength of the soldered joint [9–11].

In this paper, effect of soldering time and temperature on formation of intermetallic compounds developed between Sn–0.3Ag–0.7Cu lead-free solder and copper substrate was studied. Dip soldering was used to generate chemical reactions between the solder and the substrate. Microstructure of the intermetallic phases formed in the interfacial zone was examined and also discussed in this study.

## 2. Experimental procedures

In this experiment, Sn–0.3Ag–0.7Cu solder was melt in a graphite crucible at a selected temperature, and then a copper sheet was dipped into the molten solder for a certain time to generate chemical reaction. The melting temperature of Sn–0.3Ag–0.7Cu solder was 226 °C. The copper sheet was 99.99% in purity, and it was cleaned using a mixture of hydrochloric acid and distilled water. The cleaned copper sheet was then rinsed with ethanol, and dried in air before dipping in a flux. The flux was Almit flux RC-15SH RMA (15%). The copper sheet was then dipped into the molten solder. Dipping times used in this experiment were 5, 10, 15, and 20 s, and dipping temperatures were 250, 270, and 290 °C. The soldered specimen was cut, polished, and then etched using a solution of ethanol, nitric acid, and hydrochloric acid to reveal its microstructure.

A scanning electron microscope (SEM) was employed to examine microstructure of the interfacial zone. The SEM used in this study was JEOL model JSM-5800LV. An energy dispersive spectrometry (EDS) was used to determine chemical composition of the intermetallic phases. The EDS employed was JEOL model Link ISIS Series 300. SEM images obtained at 10,000 $\times$  was also used to measured thickness of the intermetallic phases using Image-Pro Express software. Crystal structure of the intermetallic phases was examined using an X-ray diffractometer (XRD). The XRD used for this examination was Bruker model D8-Discover. Referring to Fig. 1, the thickness of intermetallic phase ( $t$ ) was measured by summing up each area of intermetallic phase ( $A_i$ ) and then divided by the length  $L$ . This can be expressed as

\* Corresponding author at: Department of Industrial Engineering, Faculty of Engineering, King Mongkut's Institute of Technology Ladkrabang, Bangkok 10520, Thailand. Tel.: +66 2 329 8339; fax: +66 2 329 8340.

E-mail address: [kkkannac@kmitl.ac.th](mailto:kkkannac@kmitl.ac.th) (K. Kanlayasiri).

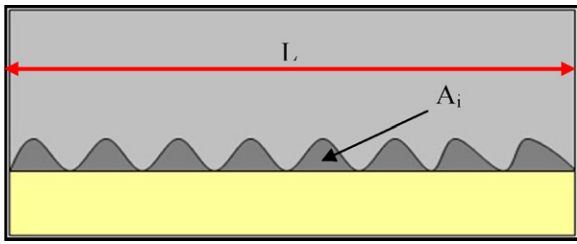


Fig. 1. Thickness measurement method.

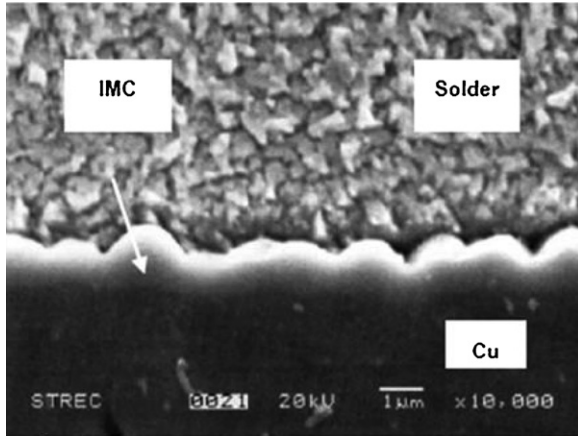


Fig. 2. Interfacial zone of soldered joint.

Eq. (1). Image-Pro Express software was used in this measurement.

$$h = \frac{\sum A_i}{L} \quad (1)$$

### 3. Results and discussion

From SEM and EDS examinations, a single layer of intermetallic compound (IMC) was observed between solder and Cu substrate as shown in Fig. 2. Two types of intermetallic phases found at the

**Table 1**  
Intermetallic phases presented at various soldering conditions.

Soldering time (s)	Soldering temperature (°C)		
	250	270	290
5	Cu <sub>3</sub> Sn	Cu <sub>6</sub> Sn <sub>5</sub>	Cu <sub>6</sub> Sn <sub>5</sub>
10	Cu <sub>3</sub> Sn	Cu <sub>6</sub> Sn <sub>5</sub>	Cu <sub>6</sub> Sn <sub>5</sub>
15	Cu <sub>6</sub> Sn <sub>5</sub>	Cu <sub>6</sub> Sn <sub>5</sub>	Cu <sub>6</sub> Sn <sub>5</sub>
20	Cu <sub>6</sub> Sn <sub>5</sub>	Cu <sub>6</sub> Sn <sub>5</sub>	Cu <sub>6</sub> Sn <sub>5</sub>

interfacial zone of the soldered joints were Cu<sub>3</sub>Sn, and Cu<sub>6</sub>Sn<sub>5</sub>. The intermetallic phases presented at the interface depended on the soldering condition, i.e., soldering time, and soldering temperature. Table 1 represents intermetallic phases found at various soldering conditions in this study. Cu<sub>3</sub>Sn was found only when the copper sheet has been soldered at 250 °C for 5 and 10 s, while Cu<sub>6</sub>Sn<sub>5</sub> was found at other soldering conditions. After soldering, Kirkendall void was not found at the interfacial zone.

From XRD analysis, Cu<sub>3</sub>Sn found at both soldering conditions was  $\epsilon$ -Cu<sub>3</sub>Sn possessing orthorhombic lattice structure while all Cu<sub>6</sub>Sn<sub>5</sub> found in this study was  $\eta$ -Cu<sub>6</sub>Sn<sub>5</sub> having hexagonal lattice structure. According to the phase diagram between Cu and Sn as shown in Fig. 3,  $\eta$ -Cu<sub>6</sub>Sn<sub>5</sub> is the intermetallic compound found at a higher temperature. However,  $\eta'$ -Cu<sub>6</sub>Sn<sub>5</sub> intermetallic phase arranging monoclinic structure which is the low-temperature Cu<sub>6</sub>Sn<sub>5</sub> phase was not found in this study. This indicated that  $\eta$ -Cu<sub>6</sub>Sn<sub>5</sub> does not transform to  $\eta'$ -Cu<sub>6</sub>Sn<sub>5</sub> during the cooling period of the soldered joint.

At a certain soldering temperature, thickness of intermetallic layers found at the interfacial zone tended to increase with soldering time as shown in Table 2. Similarly, at the same soldering time, thickness of intermetallic layer increased with soldering temperature. The increase of intermetallic layers in both cases is due to diffusional growth of these intermetallic phases during the soldering process. The growth of the intermetallic compound layer with soldering time and soldering temperature is illustrated in Fig. 4.

In this study, Cu<sub>3</sub>Sn was found only when the copper sheet has been soldered at 250 °C for 5 and 10 s while Cu<sub>6</sub>Sn<sub>5</sub> was found at higher soldering temperatures and longer soldering times. Since Cu<sub>3</sub>Sn has a lower Gibbs free energy of formation than that of

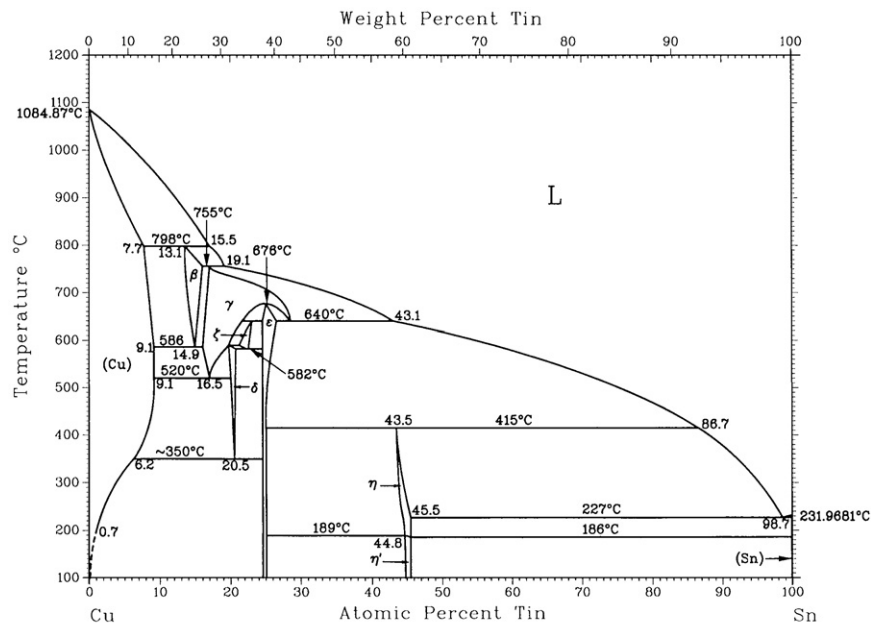


Fig. 3. Phase diagram between Cu and Sn [12].

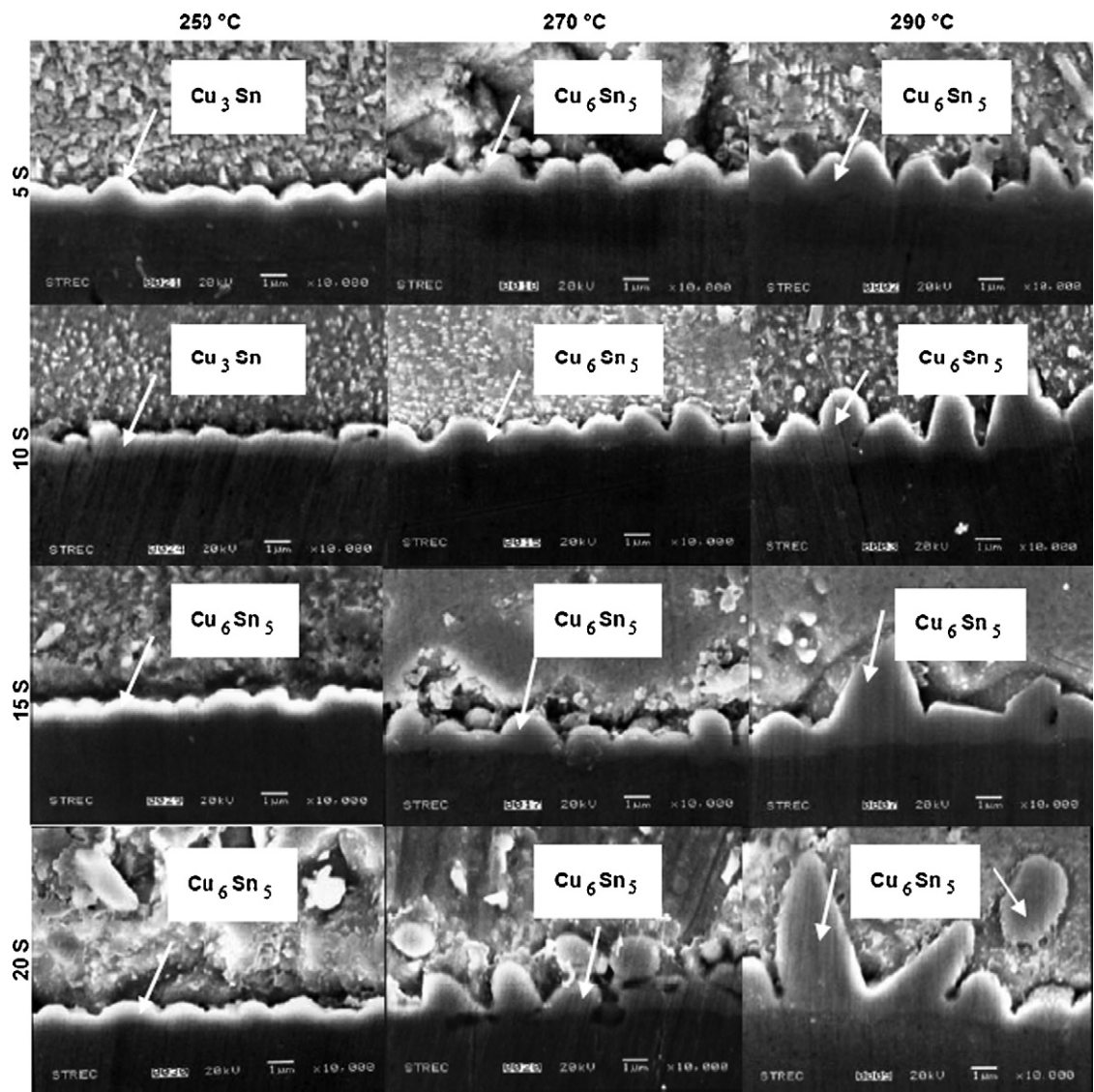


Fig. 4. Intermetallic compound found at various soldering conditions.

Cu<sub>6</sub>Sn<sub>5</sub> [13,14], therefore; Cu<sub>3</sub>Sn is easier to form at a low energy level because of this reason. In addition, at the soldering temperature of 250 °C, Cu<sub>3</sub>Sn transformed to Cu<sub>6</sub>Sn<sub>5</sub> after 10 s of the soldering time. It was reported that Cu<sub>3</sub>Sn could dissolve itself to be Cu<sub>6</sub>Sn<sub>5</sub>, and it also could react with Sn atoms to be Cu<sub>6</sub>Sn<sub>5</sub> [15,16]. The transformation equations from Cu<sub>3</sub>Sn to Cu<sub>6</sub>Sn<sub>5</sub> stated

in the literature are shown as Eqs. (2) and (3). These two reactions drove the transformation of Cu<sub>3</sub>Sn to Cu<sub>6</sub>Sn<sub>5</sub> as found at the previously mentioned soldering conditions.



**Table 2**  
Thickness of intermetallic phases at various soldering conditions.

Soldering temperature (°C)	Soldering time (s)	Intermetallic compounds	Thickness (µm)
250	5	Cu <sub>3</sub> Sn	2.07
	10	Cu <sub>3</sub> Sn	2.12
	15	Cu <sub>6</sub> Sn <sub>5</sub>	2.11
	20	Cu <sub>6</sub> Sn <sub>5</sub>	1.97
270	5	Cu <sub>6</sub> Sn <sub>5</sub>	1.33
	10	Cu <sub>6</sub> Sn <sub>5</sub>	1.64
	15	Cu <sub>6</sub> Sn <sub>5</sub>	1.76
	20	Cu <sub>6</sub> Sn <sub>5</sub>	1.92
290	5	Cu <sub>6</sub> Sn <sub>5</sub>	1.93
	10	Cu <sub>6</sub> Sn <sub>5</sub>	2.02
	15	Cu <sub>6</sub> Sn <sub>5</sub>	2.16
	20	Cu <sub>6</sub> Sn <sub>5</sub>	2.35

It is recalled that Cu<sub>3</sub>Sn and Cu<sub>6</sub>Sn<sub>5</sub> found in this study possessed orthorhombic and hexagonal lattice structure, respectively. It is well known that mechanical properties of materials also depend on their lattice structure. Different lattice structure possesses different number of slip systems, and consequently reveals different mechanical properties [17]. This implies that mechanical properties of soldered joint between Sn–0.3Ag–0.7Cu solder and copper substrate tends to change with soldering condition because of the occurrence of different intermetallic phases at the interface. Generally, Cu<sub>3</sub>Sn provides a less reliable soldered joint when diffusion of Cu and Sn atoms takes place in the joint because the Kirkendall voids will form at the interface between Cu<sub>3</sub>Sn layer and Cu substrate, and these voids could lead to a brittle fracture of the joint while Cu<sub>6</sub>Sn<sub>5</sub> does not induce the Kirkendall voids formation [18–22]. Therefore, based on the reliability of the joint, Cu<sub>6</sub>Sn<sub>5</sub> is preferred to Cu<sub>3</sub>Sn. However, it was found from this study that

the preferred intermetallic phase  $\text{Cu}_6\text{Sn}_5$  occurred at the interfacial zone only when soldered with a higher energy, and it is well known that soldering with a higher energy could damage the electronics devices and circuit board. Moreover, it should be noted that  $\text{Cu}_6\text{Sn}_5$  could also develop to  $\text{Cu}_3\text{Sn}$  if the joint is used under service condition like a thermal aging [18–22].

#### 4. Summary

Effect of soldering condition on formation of intermetallic compounds developed between  $\text{Sn}-0.3\text{Ag}-0.7\text{Cu}$  lead-free solder and copper substrate was investigated in this study. Either  $\varepsilon\text{-Cu}_3\text{Sn}$  or  $\eta\text{-Cu}_6\text{Sn}_5$  intermetallic phase was found at the interface between the solder and the substrate depending on the soldering condition, i.e., soldering time and soldering temperature.  $\varepsilon\text{-Cu}_3\text{Sn}$  was found only at a lower soldering energy when the substrate was soldered at  $250^\circ\text{C}$  for 5 and 10 s. At other soldering conditions, only  $\eta\text{-Cu}_6\text{Sn}_5$  was found at the interfacial zone. Crystal structure of  $\varepsilon\text{-Cu}_3\text{Sn}$  intermetallic phase was orthorhombic, and it was hexagonal structure for  $\eta\text{-Cu}_6\text{Sn}_5$ . In addition,  $\varepsilon\text{-Cu}_3\text{Sn}$  was able to transform to be  $\eta\text{-Cu}_6\text{Sn}_5$  at certain soldering conditions.

#### Acknowledgements

The authors would like to thank Faculty of Engineering, King Mongkut's Institute of Technology Ladkrabang and Office of the National Research Council of Thailand for the financial support of this research.

#### References

- [1] M. Amagai, Y. Toyoda, T. Ohnishi, S. Akita, Electronic Components and Technology Conference, 2004, pp. 1304–1309.
- [2] K.S. Kim, K. Suganuma, Third International Symposium on Environmentally Conscious Design and Inverse Manufacturing, 2003, pp. 414–415.
- [3] F. Zhu, H. Zhang, R. Guan, S. Liu, Journal of Alloys and Compounds 438 (2007) 100–105.
- [4] Y. Fukuda, P. Casey, M. Pecht, IEEE Transactions on Electronics Packaging Manufacturing 26 (2003) 305–312.
- [5] K.S. Kim, S.H. Huh, K. Suganuma, Journal of Alloys and Compounds 532 (2003) 226–236.
- [6] F. San, P. Hochstenbach, W.D. Van Driel, G.Q. Zhang, Microelectronics Reliability 48 (2008) 1167–1170.
- [7] M.P. Groover, Fundamentals of Modern Manufacturing: Materials, Processes, and Systems, 3rd edition, John Wiley & Sons Inc., 2007.
- [8] A.R. Zbrzezny, P. Saugovsky, D.D. Perovic, Microelectronic Reliability 47 (2007) 2205–2214.
- [9] P. Limaye, B. Vandeveld, R. Labie, D. Vandepitte, B. Valinden, IEEE Transactions on Advanced Packaging 31 (2008) 51–57.
- [10] K.S. Kim, S.H. Huh, K. Suganuma, Journal of Alloys and Compounds 352 (2003) 226–236.
- [11] F. San, P. Hochstenbach, W.D. Van Driel, G.Q. Zhang, Microelectronic Reliability 48 (2008) 1167–1170.
- [12] T.B. Massalski, H. Okamoto, Binary Alloy Phase Diagrams, 2nd edition, ASM International, 1990.
- [13] H. Yu, V. Vuorinen, J. Kivilahti, Electronic Component and Technology Conference, 2006, pp. 1204–1209.
- [14] R. Hultgren, P.D. Desai, D.T. Hawkins, M. Gileiser, K.K. Kelly, Selected Values of the Thermodynamic Properties of Binary Alloys, ASM, 1973.
- [15] Paul, A., The Kirkendall Effect in Solid State Diffusion, Ph.D. Thesis, Eindhoven University of Technology, The Netherlands, 2004.
- [16] C. Yu, H. Lu, S. Li, Journal of Alloys and Compounds 460 (2008) 594–598.
- [17] W.D. Callister, D.G. Rethwisch, Materials Science and Engineering, 8th edition, John Wiley & Sons Inc., 2011.
- [18] D.Q. Yu, C.M.L. Wu, C.M.T. Law, L. Wang, J.K.L. Lai, Journal of Alloys and Compounds 392 (2005) 192–199.
- [19] C.E. Ho, S.C. Yang, C.R. Kao, Journal of Materials Science: Materials in Electronics 18 (2007) 155–174.
- [20] W. Peng, E. Monlevade, M.E. Marques, Microelectronic Reliability 47 (2007) 2161–2168.
- [21] G.T. Lim, B.J. Kim, K. Lee, J. Kim, Y.C. Joo, Y.B. Park, Journal of Electronic Materials 38 (2009) 2229–2233.
- [22] G. Zeng, S. Xue, L. Zhang, L. Gao, W. Dai, J. Luo, Journal of Materials Science: Materials in Electronics 21 (2010) 421–440.